LANL C-band Engineering Research Facility (CERF-NM)

CERF-NM was built with $3M of LANL's internal infrastructure investment.

- Powered with a C-band Canon klystron
- Conditioned to 50 MW
- Frequency 5.712 GHz
- 300 ns – 1 μs pulse length
- Rep rate up to 200 Hz (typical 100 Hz)
- Nominal bandwidth 5.707-5.717 GHz

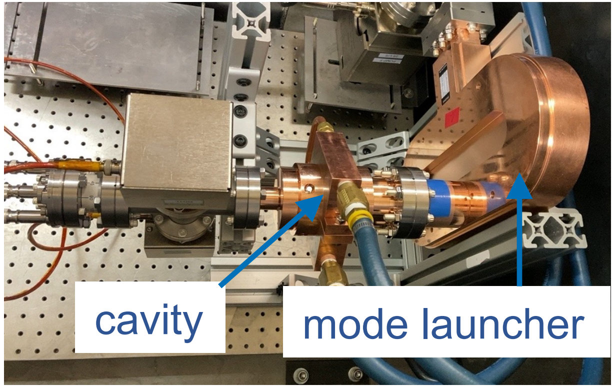

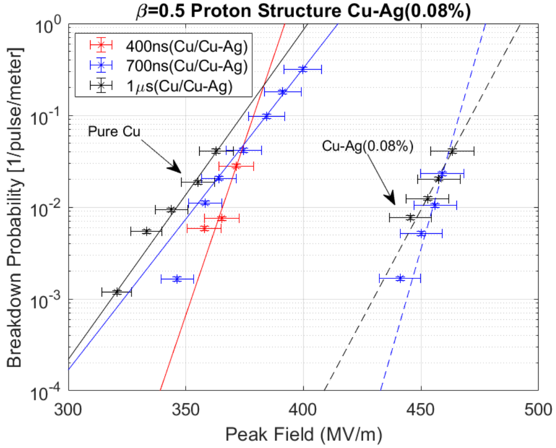

LDRD
LABORATORY DIRECTED
RESEARCH & DEVELOPMENT

LANL has plans for further developing its C-band accelerator capabilities

- We aim to develop a C-band accelerator test facility for advanced cathode, accelerator, and material studies.
- A location was identified on LANSCE mesa that can accommodate a 20 kW electron beam.
- Director Initiative money were allocated in FY22 to jump start this facility.
- 5-year goal: build operational C-band cryo-cooled copper accelerator.
- Ultimate goal: provide 43 keV photon bursts for material studies

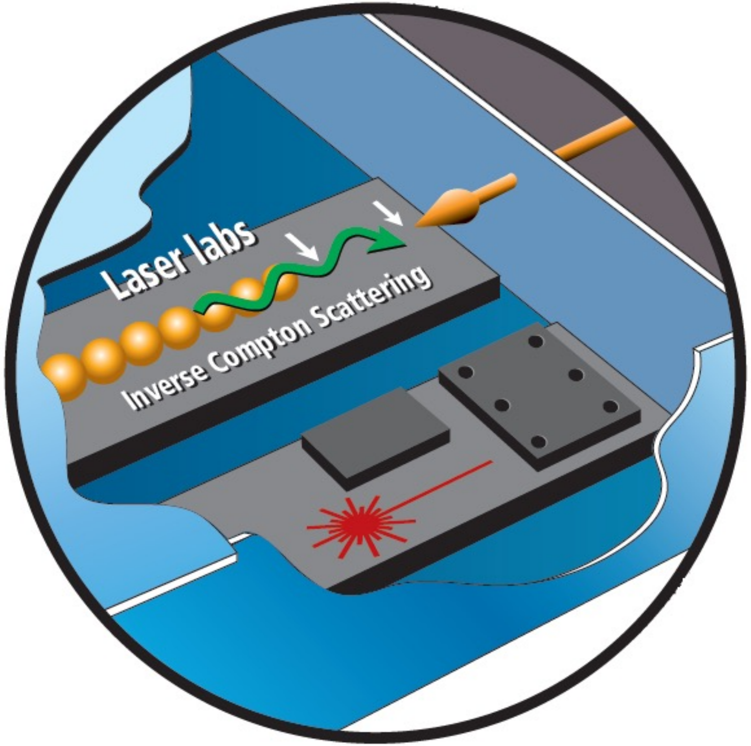

LABORATORY DIRECTED RESEARCH & DEVELOPMENT

LANL new project: Cathodes and Rf Interactions in Extremes (CARIE)

- A new three-year project was funded at LANL to demonstrate operation of high-quantum-efficiency cathode in a high-gradient RF injector.
- Project builds upon LANL's expertise in high-gradient C-band and high-QE photocathodes.
- The proposed heterostructured cathode will include multiple layers to ensure atomic flatness of the surface, high QE, and the ability to withstand high electric fields with no breakdown.
- Target beam parameters: 250 pC, 0.1 mm*rad
- TBD: RF gun geometry, gradient, final beam energy, materials

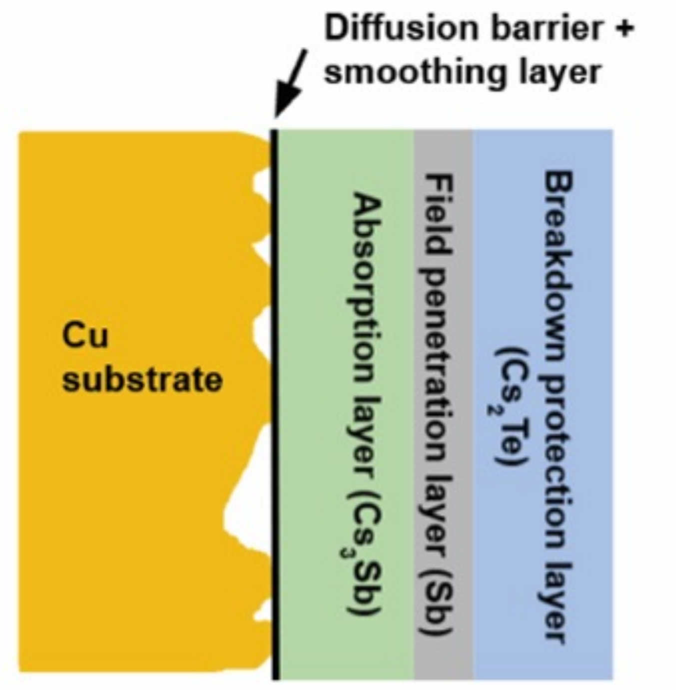

LDRD
LABORATORY DIRECTED RESEARCH & DEVELOPMENT

C^3 Demonstrator Cryogenics and Layout

Martin Breidenbach, Emilio Nanni, Marco Oriunno, Caterina Vernieri

Snowmass

July 2022

U.S. DEPARTMENT OF ENERGY Office of Science

SLAC NATIONAL ACCELERATOR LABORATORY

Functionality

- Mode 1 - Normal Accelerator development
  - LN at nominal height above accelerator sections
  - low LN flow
- Mode 2 - High flow for vibration testing etc, up to 10 kg/sec

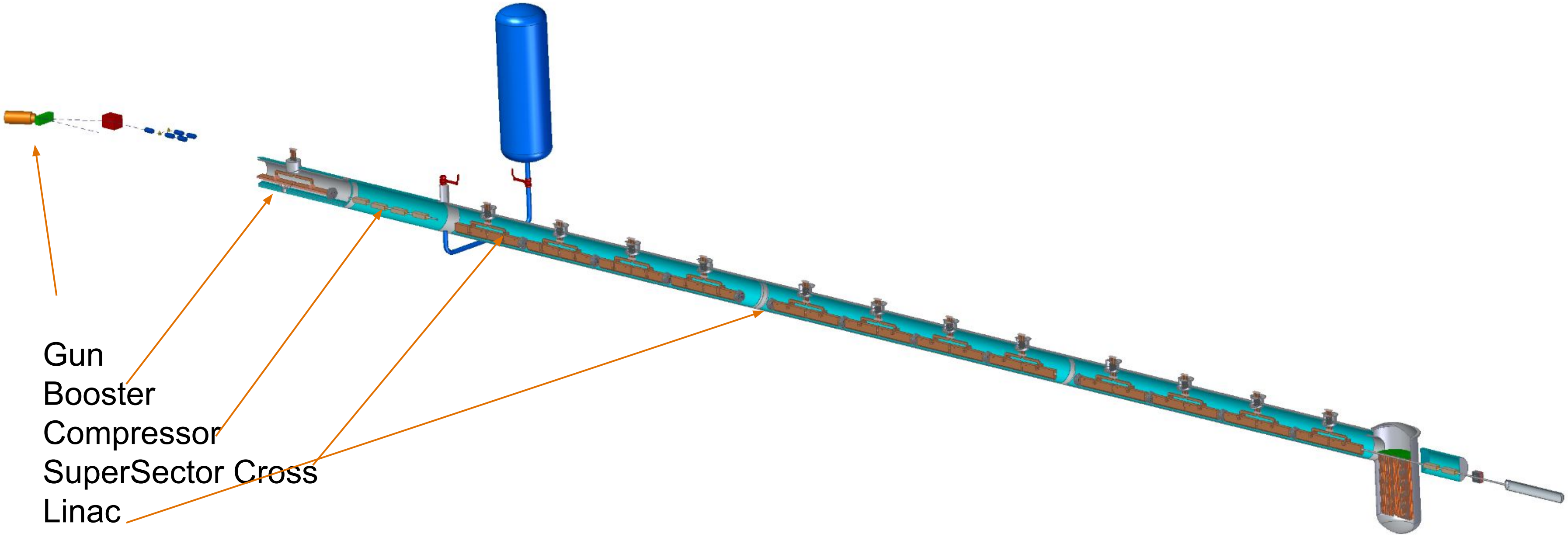

Simplified Cryogenic Layout

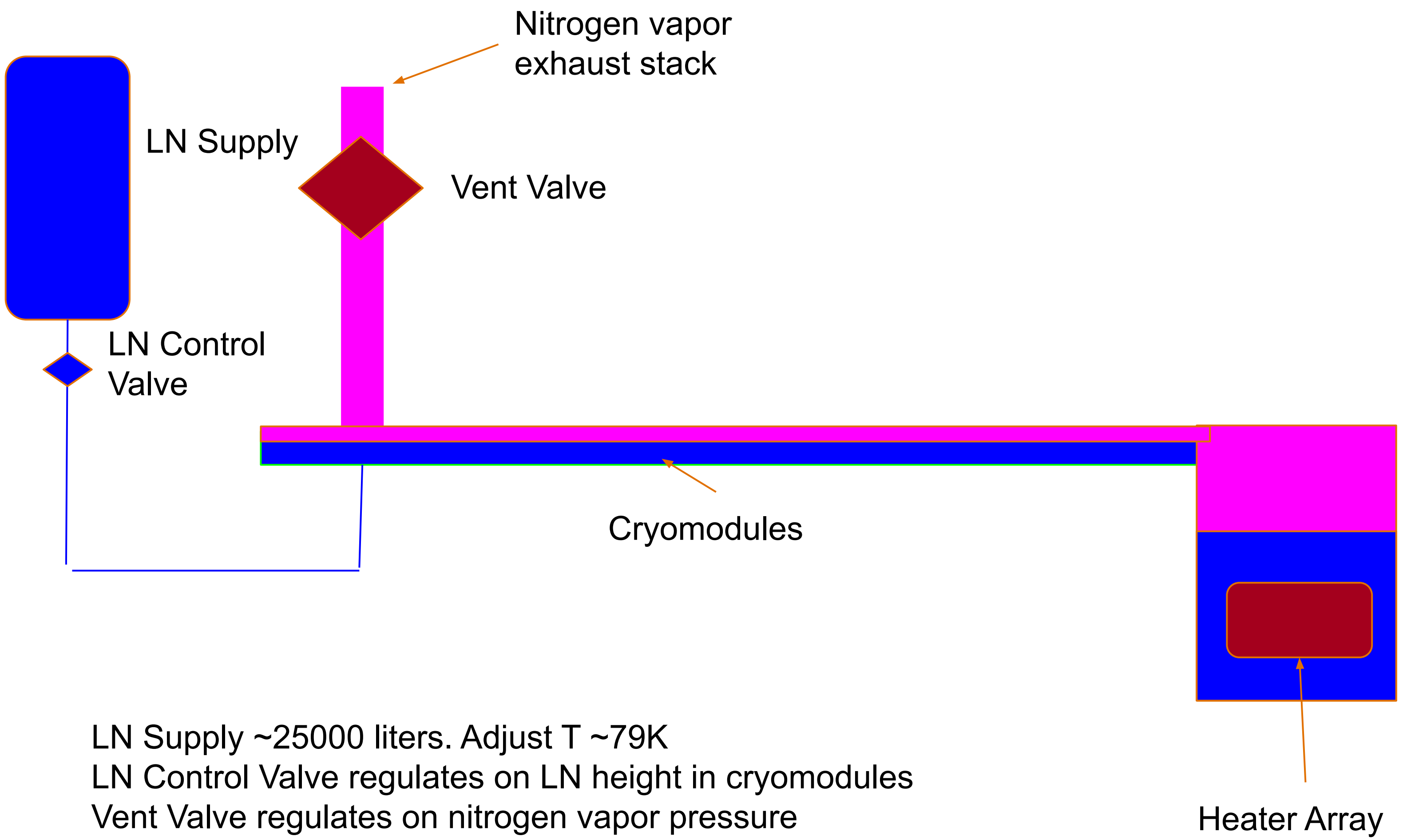

LN Supply ~25000 liters. Adjust T ~79K
LN Control Valve regulates on LN height in cryomodules
Vent Valve regulates on nitrogen vapor pressure

LN in, vapor out at "SuperSector Cross"

LN comes in from bottom, inlet control valve regulates on liquid level.

Outlet valves regulates on pressure of vapor in cryomodules.

Both may require some feed-forward.

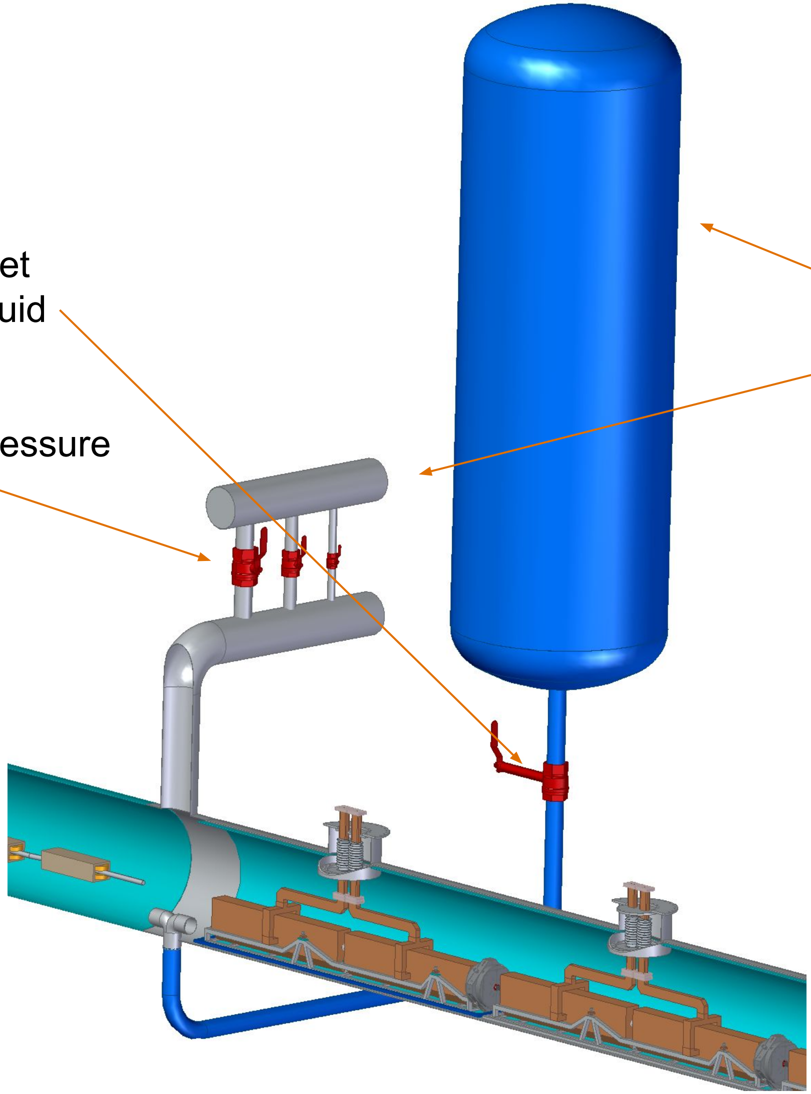

LN Tank ~25000 liters
Vent stack need to go suitably far away, as in over the hill

Boiler

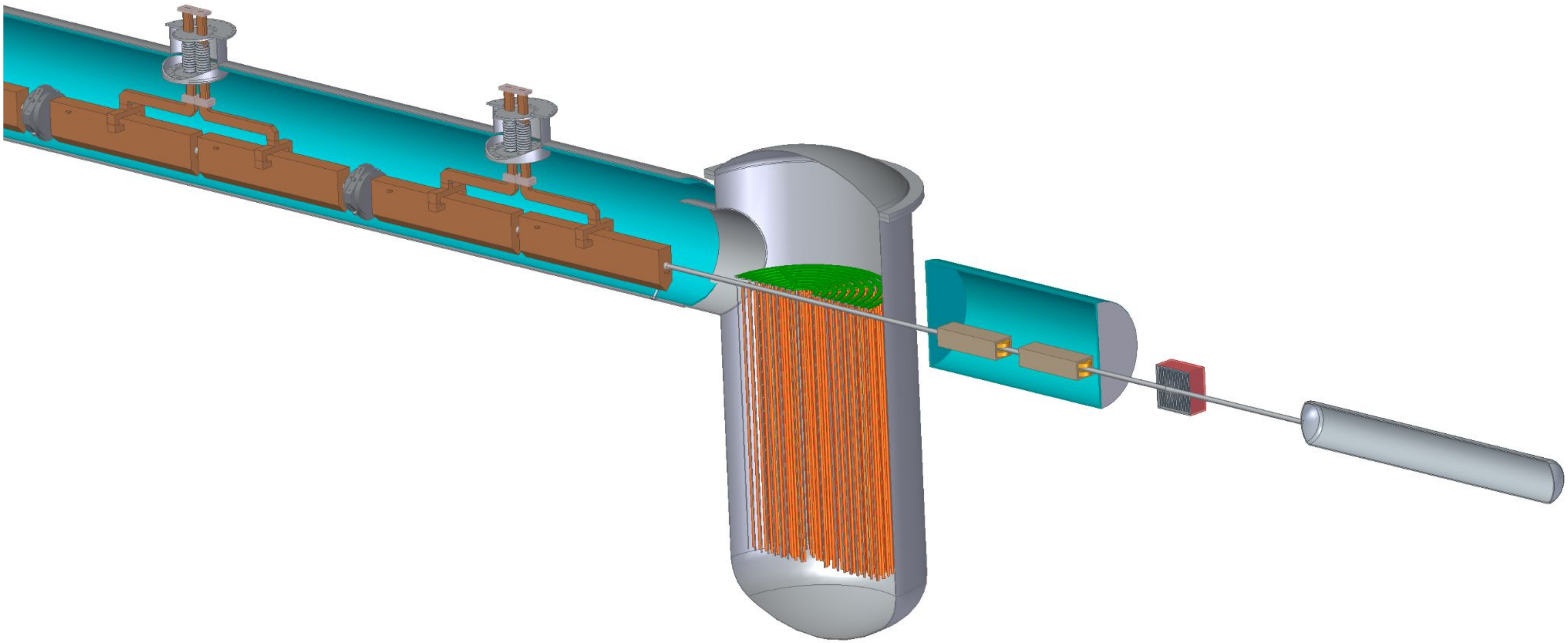

LN in boiler at same level as in cryomodules, covering Calrod array.

GUO CRYOGENICS LAB

Our facilities:

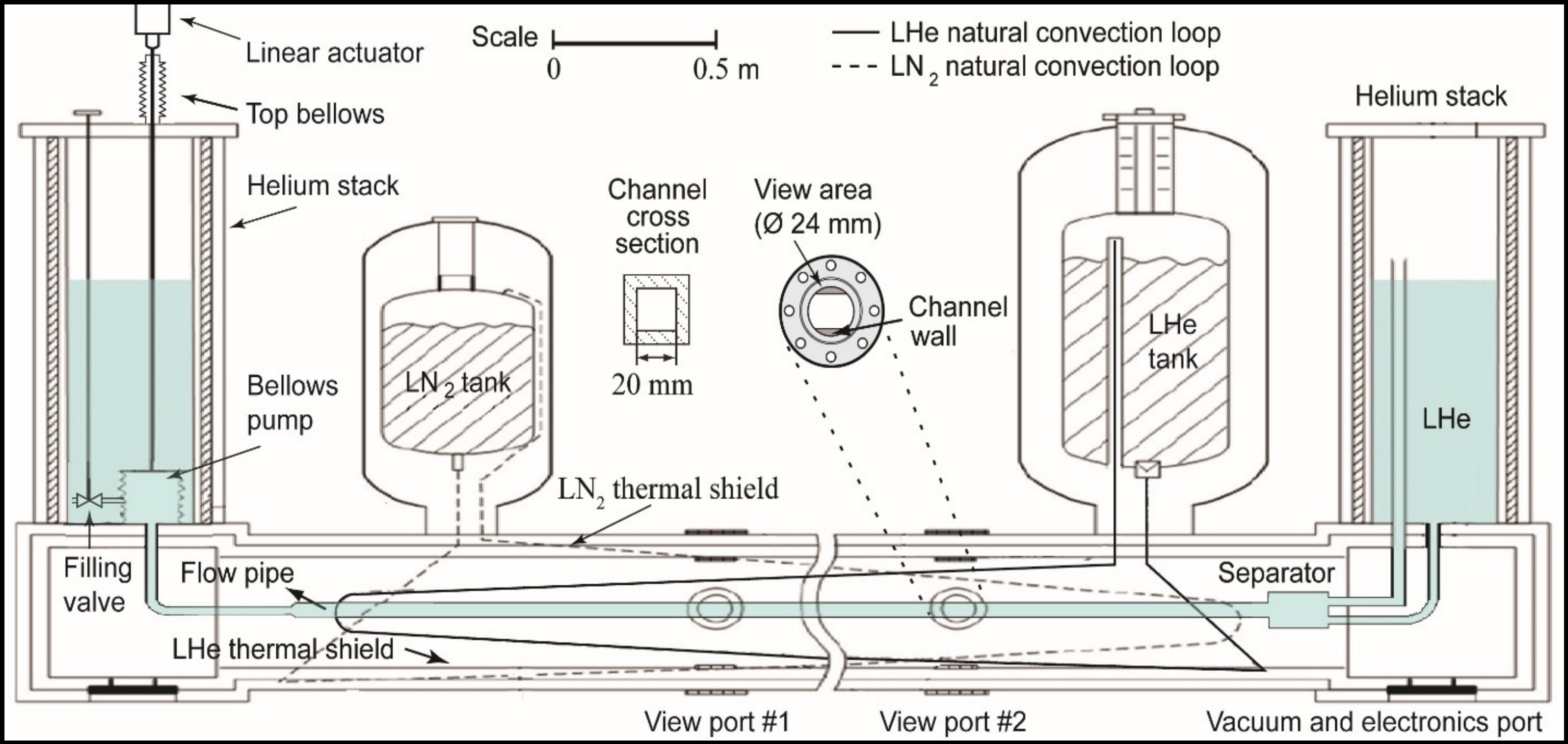

Our unique strength:

Powerful quantitative flow visualization measurement capability in cryogenic fluids:

- Molecular tagging velocimetry:

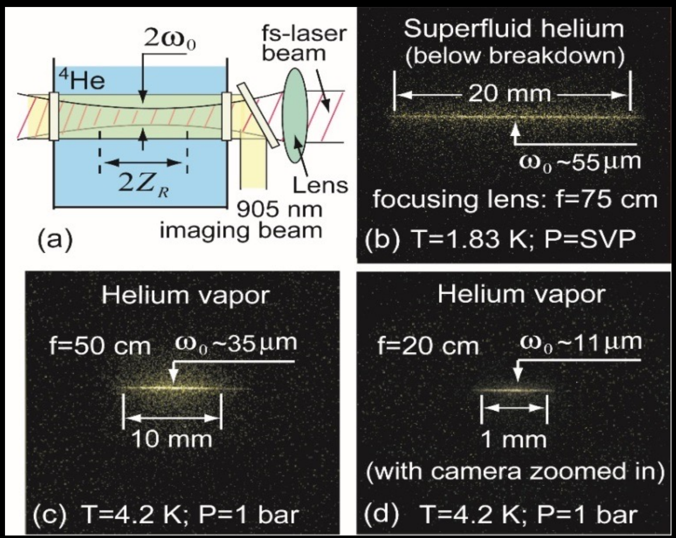

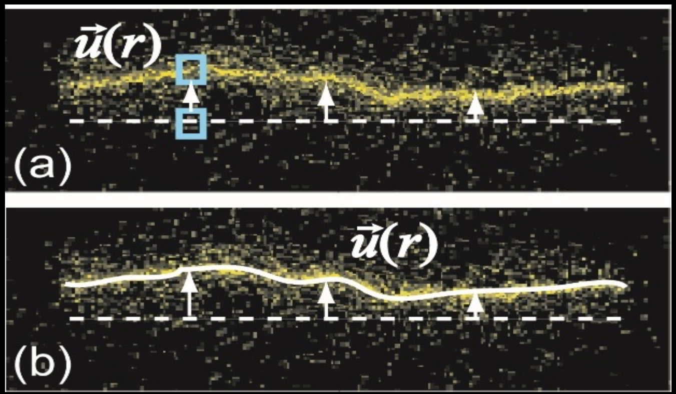

- W. Guo, *et al.*, PNAS, 111, 4653 (2014)
- A. Marakov, et al., PRB 91, 094503 (2015)
- J. Gao, et al, PRB, 97, 184518 (2018)
- T. Kanai, PRL, 127, 095301 (2021)

- Particle tracking velocimetry:

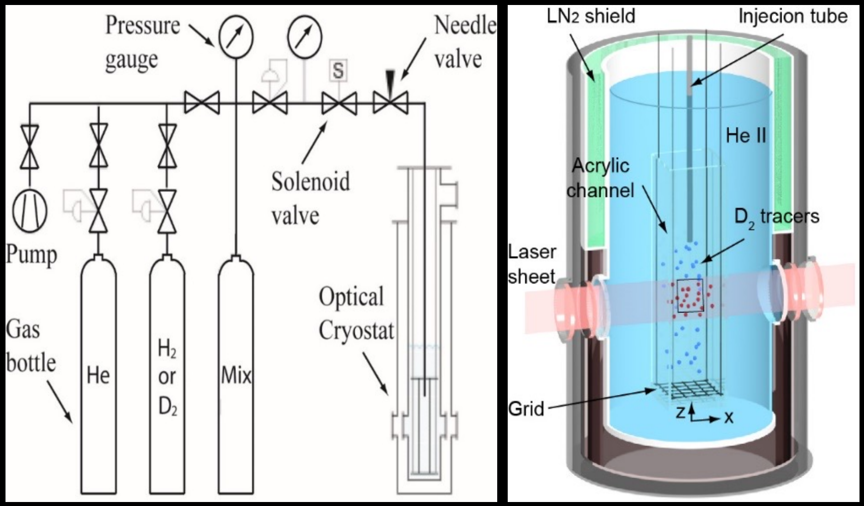

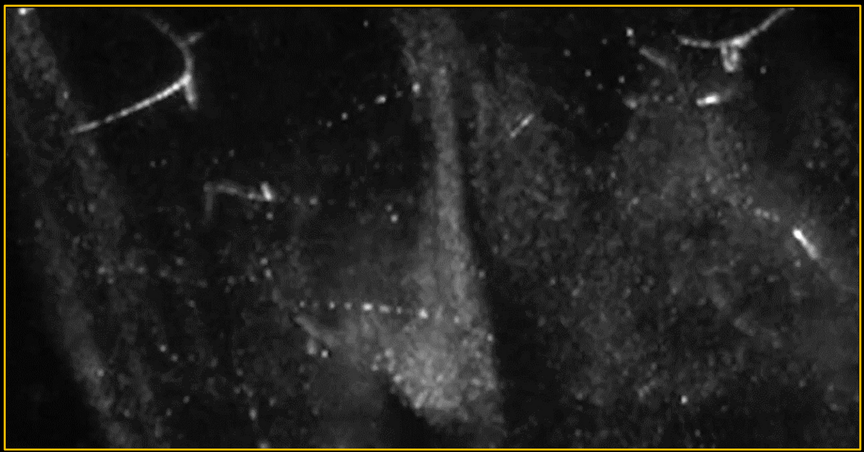

- S. Yui, et al., PRL., 124, 155301 (2020).
- Y. Tang, et al., PNAS, 118, e2021957118, (2021)
- S. Yui, et al., PRL., 129, 025301 (2022)

Existing R&D work pertinent to particle accerlerator cryogenics

(1) Heat/mass transfer during loss-of-vacuum accident for cryogenic systems.

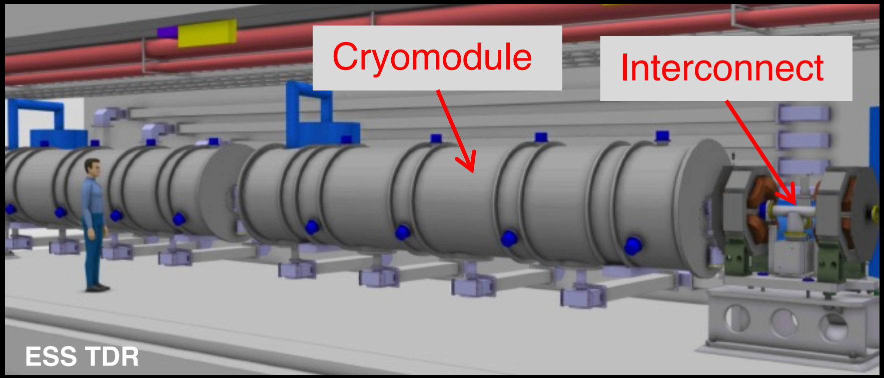

PI: Guo

- 03/2022 -06/2023 (renewal)
  Amount: $675,000
- 04/2019 - 03/2022;
  Amount: $600,000
- 04/2016 - 03/2019;
  Amount: $765,000

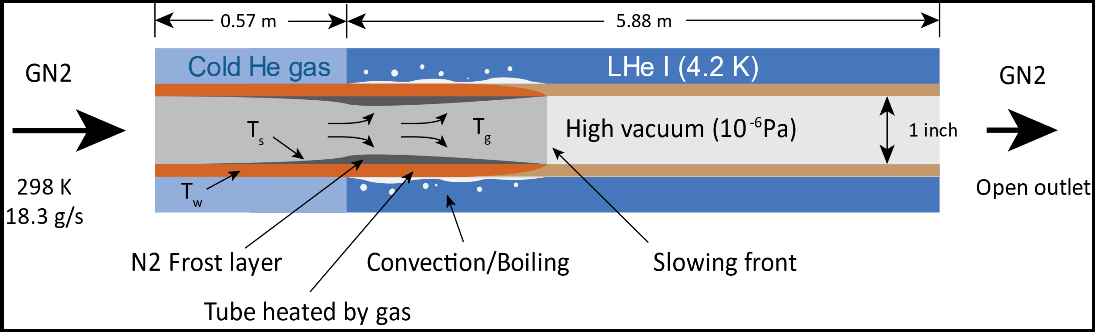

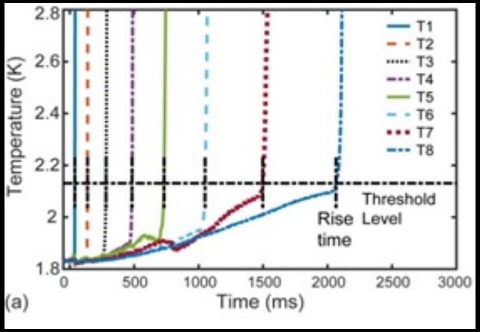

- N. Garceau, S. Bao, W. Guo, Int. J. Heat Mass Tran., 181, 121885 (2021)
- S. Bao, N. Garceau, and W. Guo, Int. J. Heat Mass Tran., 146, 118883 (2020)
- N. Garceau, S. Bao, W. Guo, S.W. Van Sciver, Cryogenics, 100, 92 (2019)
- N. Garceau, S. Bao, and W. Guo, Int. J. Heat Mass Tran., 129, 1144 (2019)

Knowledge gained could guide the design and safe operation accelerator cryogenic systems

(2) SRF cavity quench spot detection:

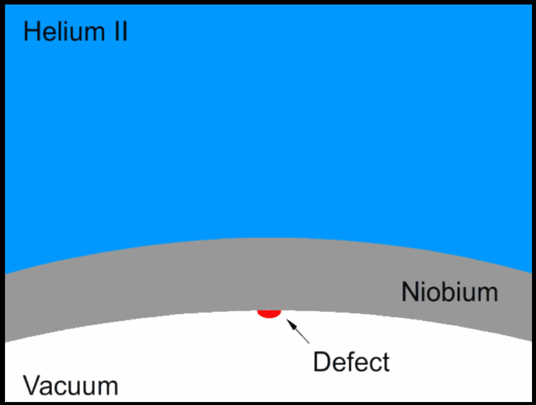

- SRF cavities, cooled by He II, are critical components of modern particle accelerators.
- The maximum accelerating field is limited by cavity quenching caused by heating from tiny defects on the inner surface.

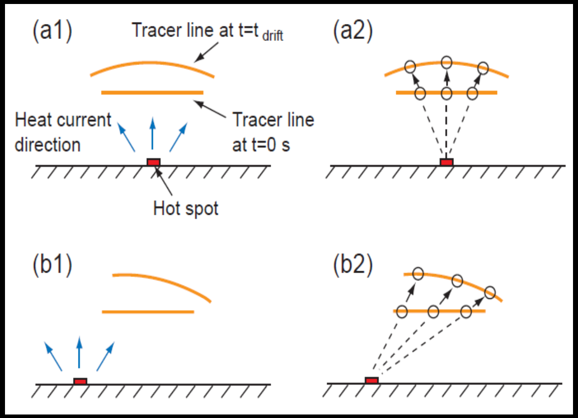

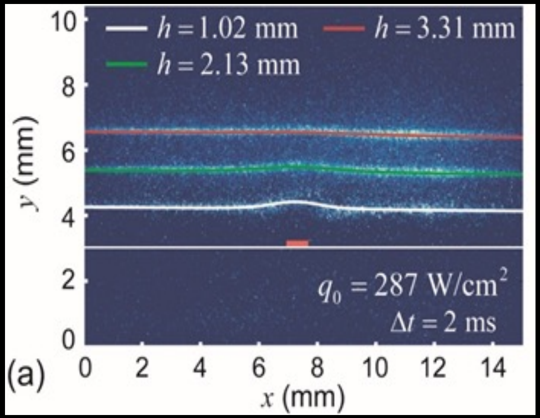

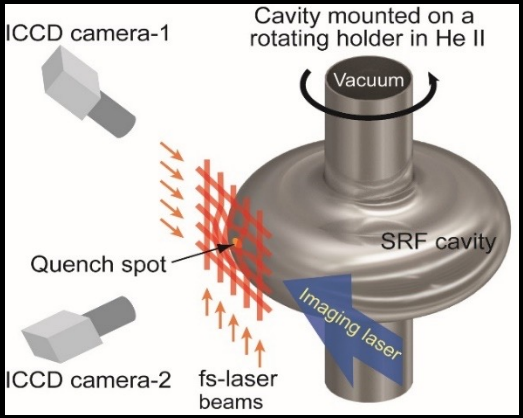

- S. Bao and W. Guo, Phys. Rev. Applied, 11, 044003 (2019)
- S. Bao et al., Int. J. Heat Mass Trans., 161, 120259 (2020)

Our flow visualization-based quench spot detection technique has demonstrated superior spatial resolution, i.e., ~ 10^2 microns.

Overview of computational capabilities

Multimaterial/multiphase systems

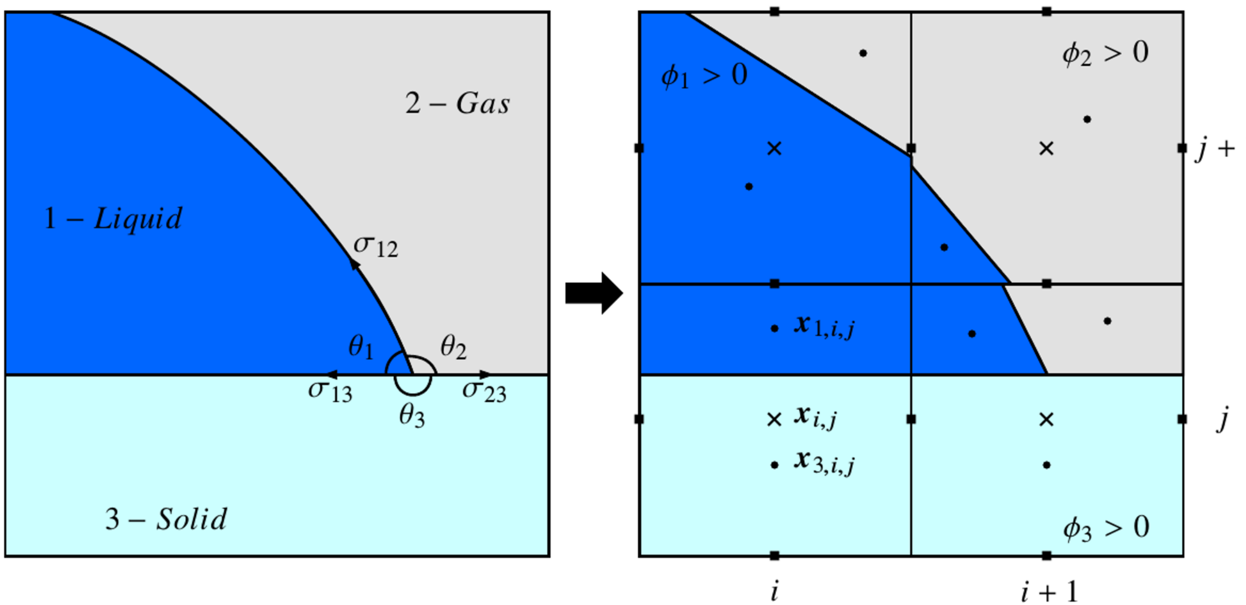

Fluid-structure interaction for flexible/rigid geometries

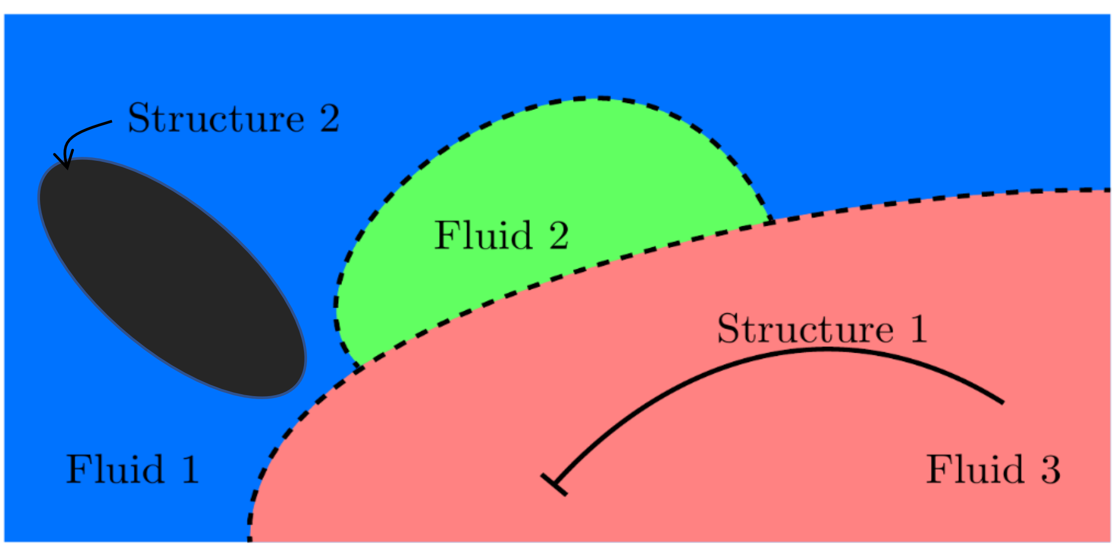

Adaptive Mesh Refinement (AMR)

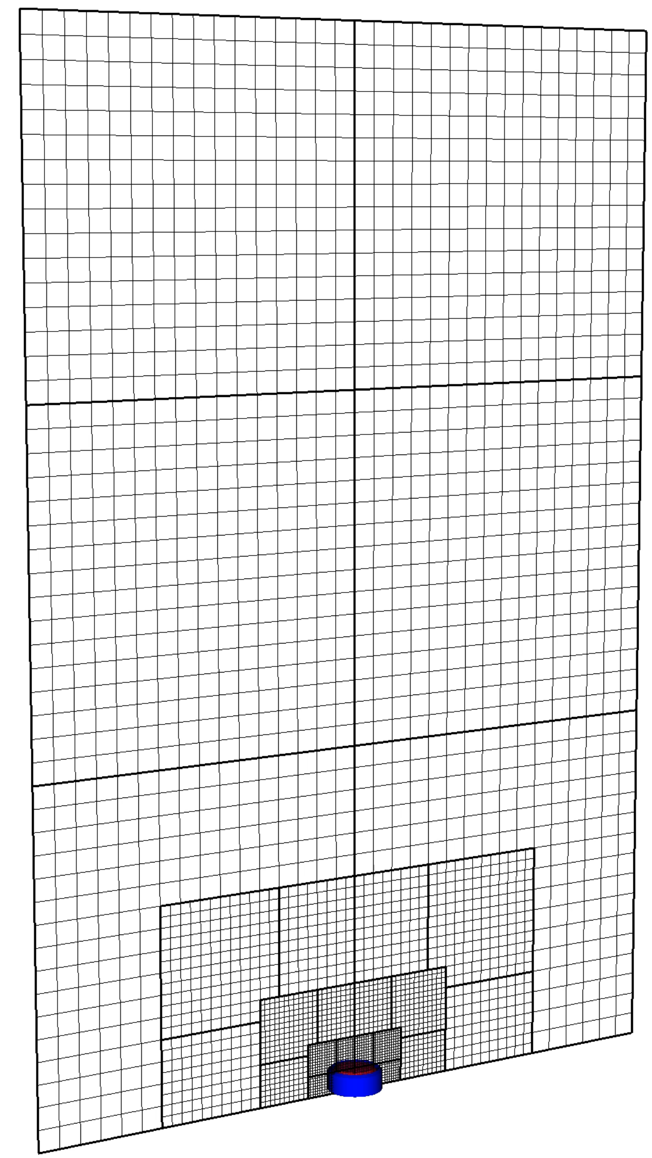

Overview of computational capabilities

Surface tension dynamics and flows

Bubble formation from a nozzle under water

Water and diesel drop impact

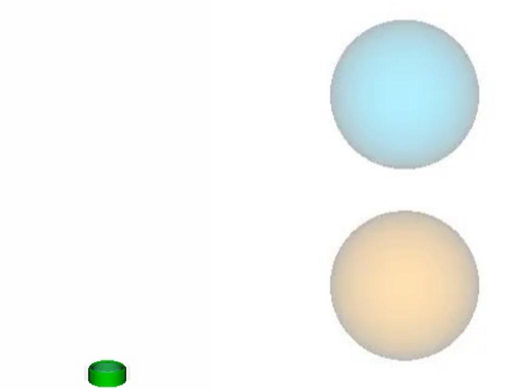

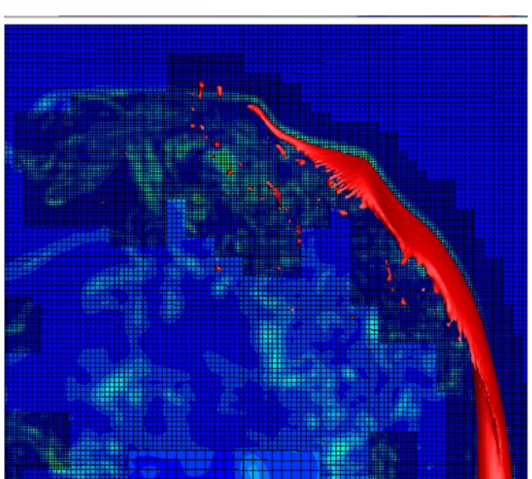

Phase-change dynamics: Solidification/melting

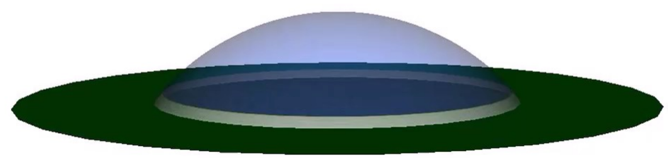

Droplet solidification on a flat surface

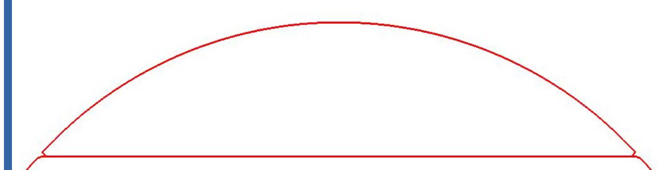

Dependency of droplet shape on surface tension coefficients

Phase-change dynamics: Boiling/condensation

Nucleate pool boiling from a hot substrate

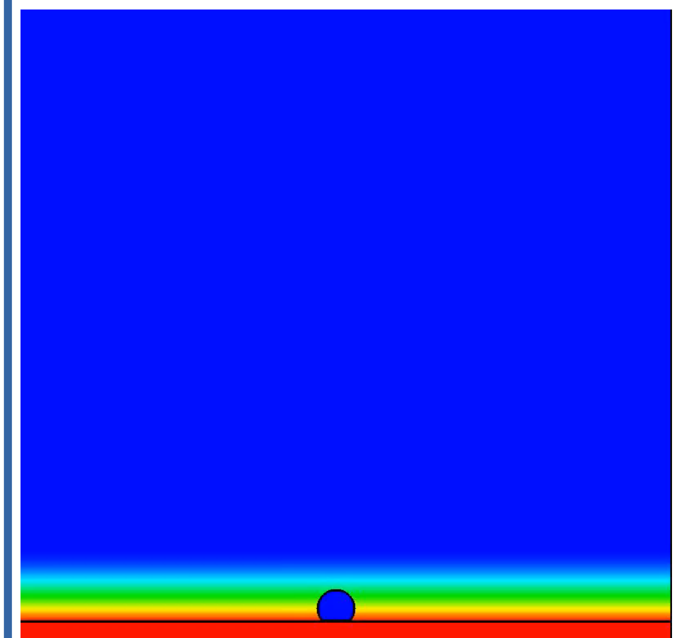

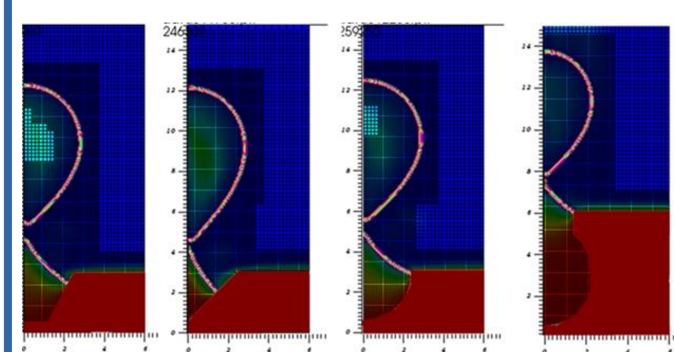

Cryogenic flow simulations

Storage tank

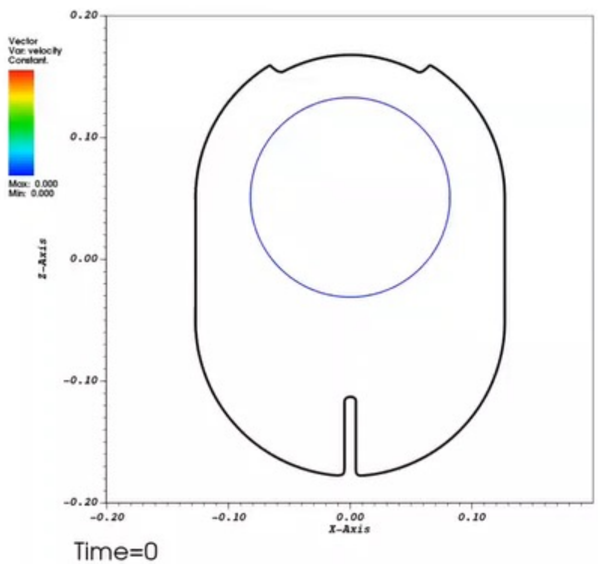

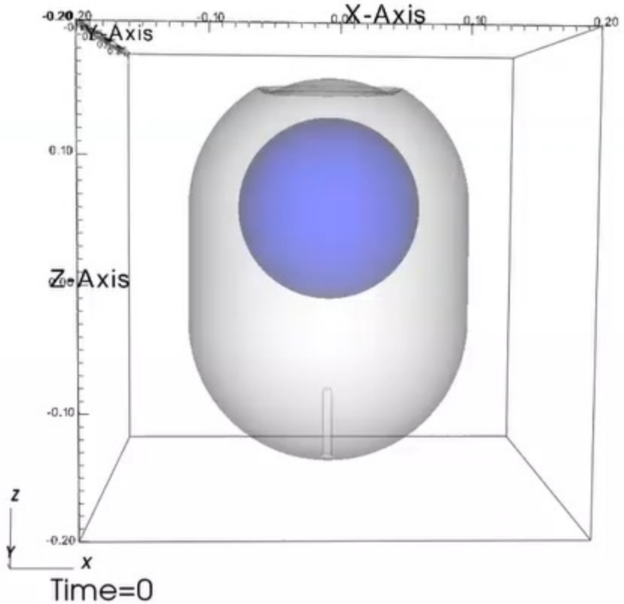

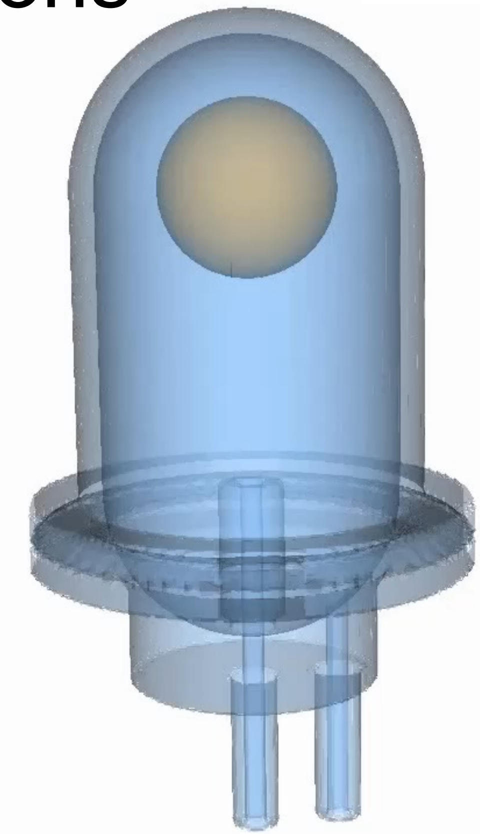

Evaporation

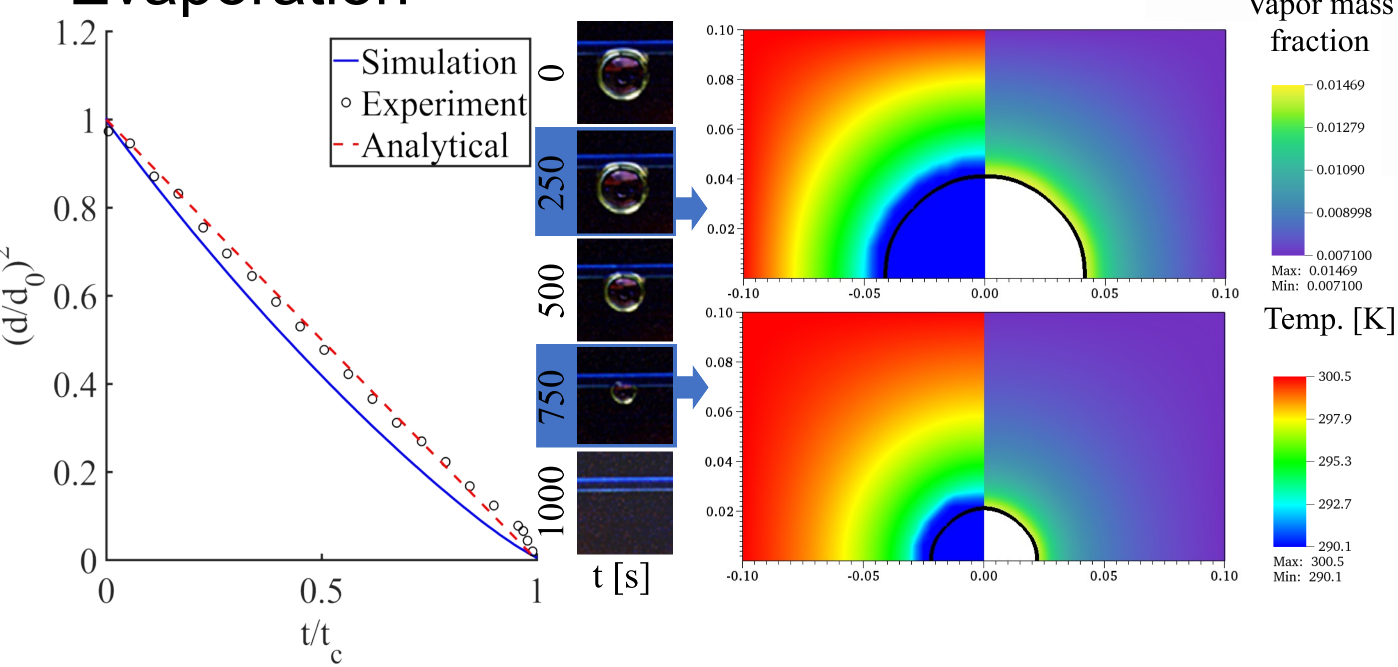

Water drop evaporation at room temperature. a) Comparison of the drop diameter for the simulations, experimental and analytical results $\left(\frac{d}{d_0}\right)^2 = -\frac{t}{t_c} + 1$, b) Experimantal results for a droplet of diameter 1mm, c) Corresponding vapor mass fraction and temperature field in the simulation.

Our Potential Contributions

Liquid gas interface dynamic with evaporation

- Characterization of the maximum gas velocity without the large surface waves
- Enhanced heat transfer/evaporation due to the surface motion
- Short-time and long-time prediction of the surface motion

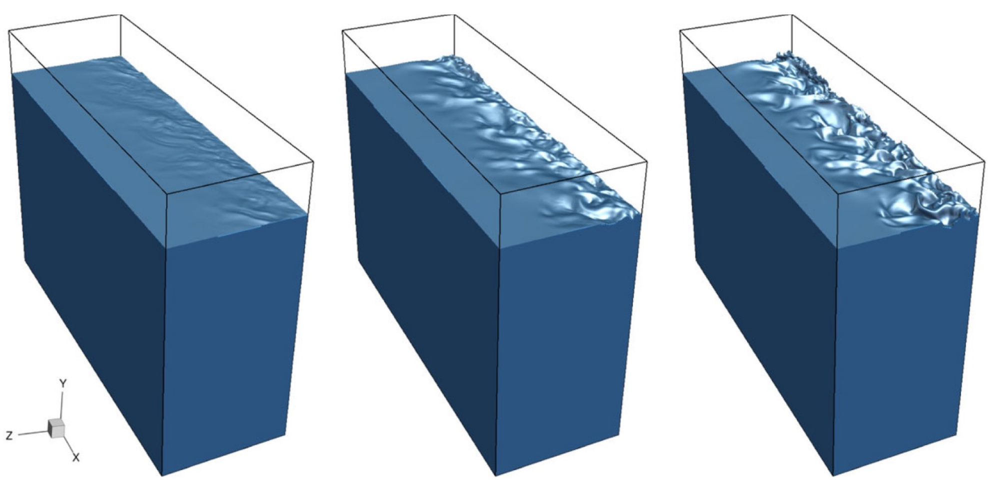

Nasiri, Balaras 2020

Nucleate boiling

- Boundary orientation and surface conditions

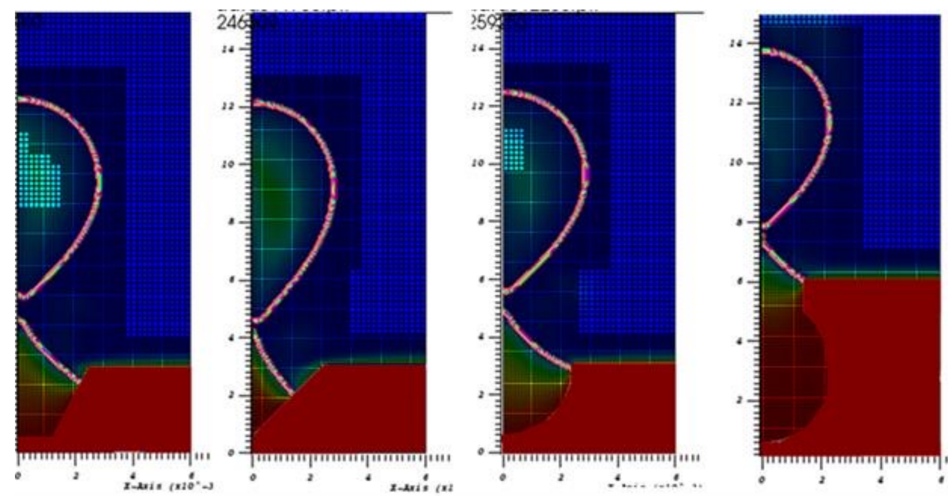

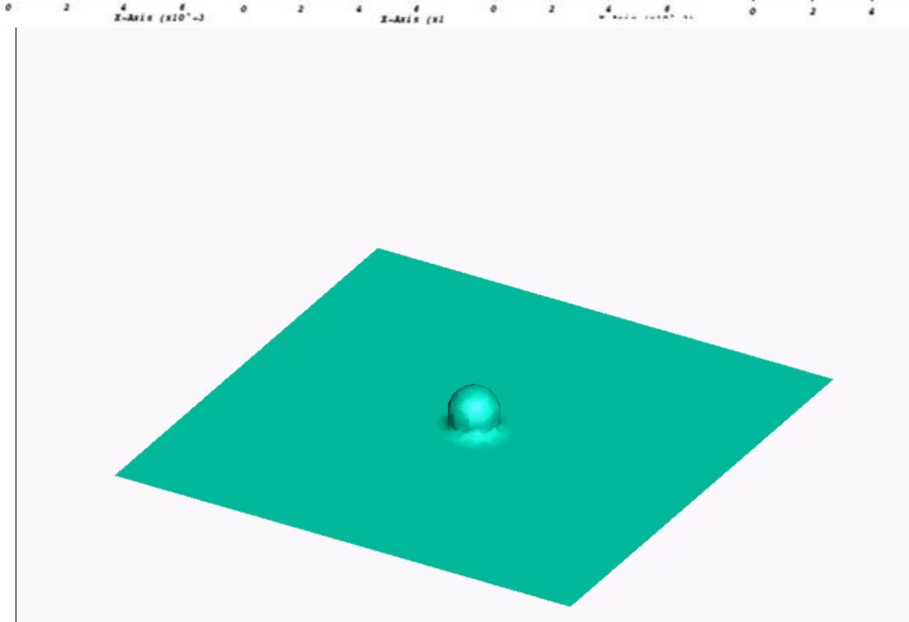

LINAC LN Vibration Emulation Test Bed

Laser Micrometer

RTD Temperature Sensor

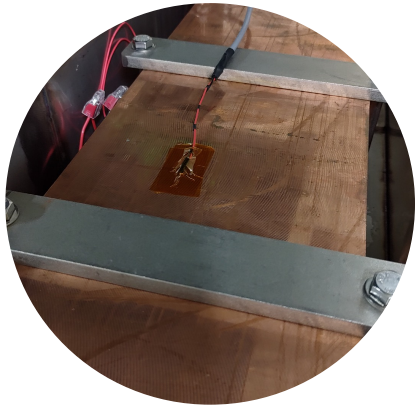

Accelerometers

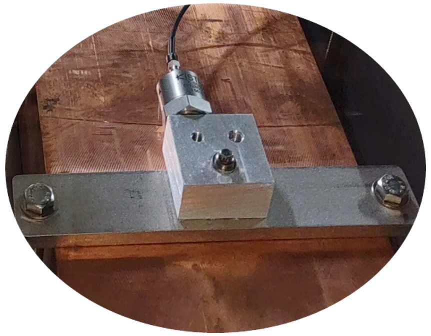

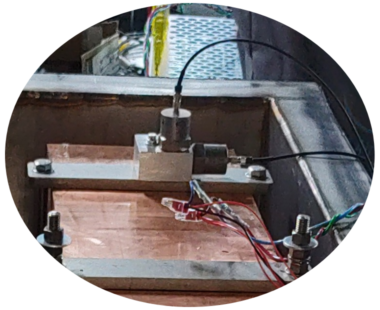

Vibrational Analysis on the Test Bed

Knock test to initiate self-resonances in the structure

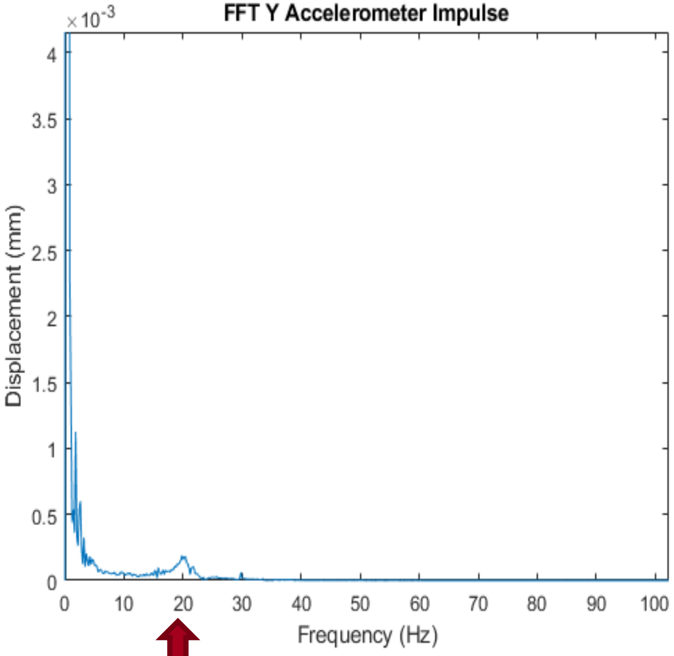

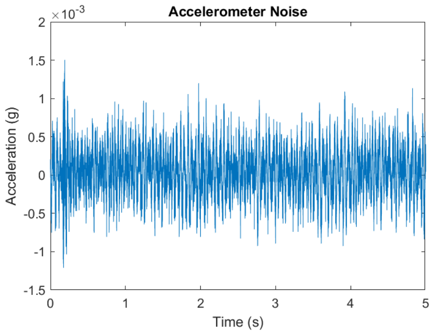

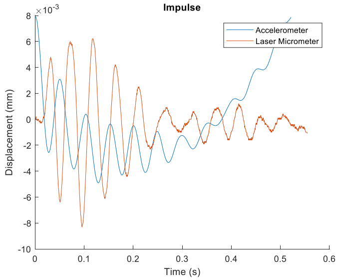

Knock Calibration

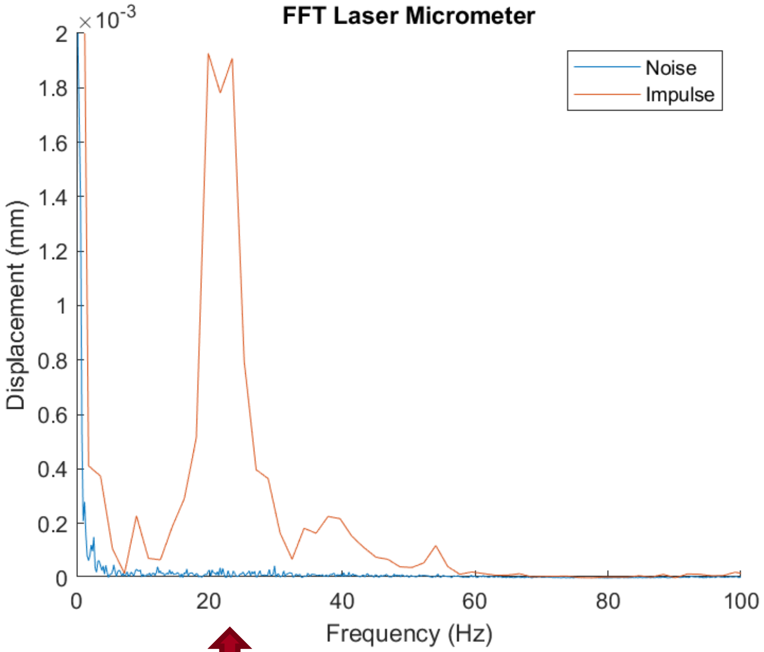

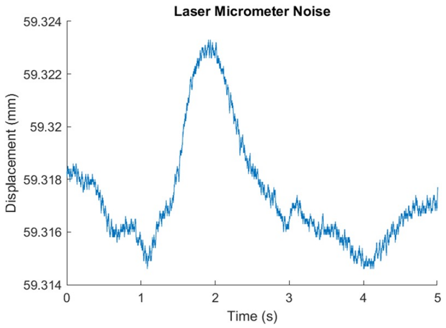

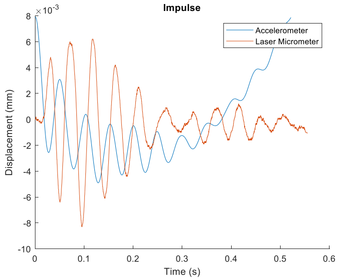

Knock Calibration

Laser micrometer and accelerometer measurement at the room temperature.

Vibrational Analysis on the Test Bed

Low temperature LN bubbling initiated vibrations of the structure

Laser micrometer measurements

Full level of LN

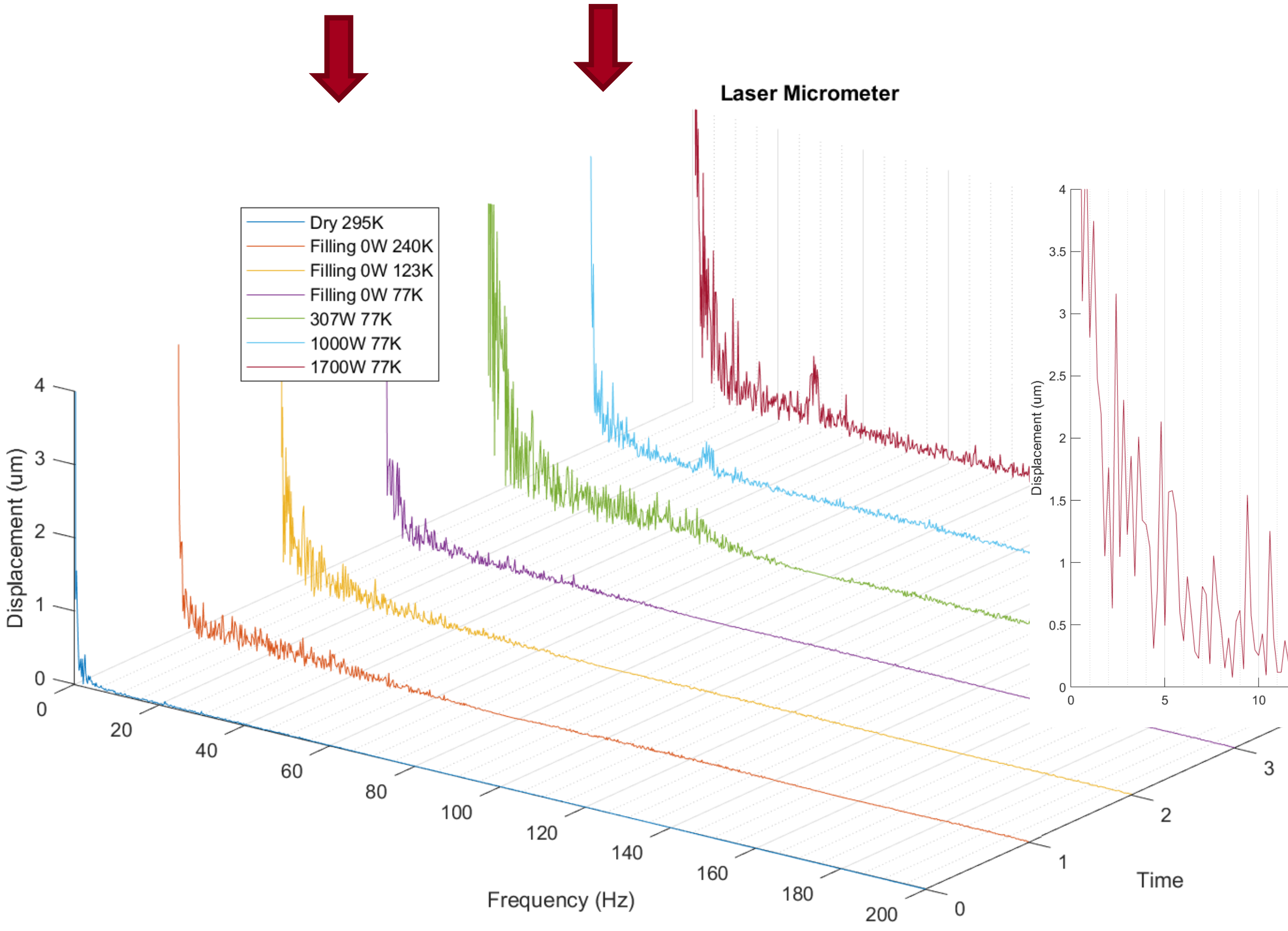

MAX POWER APPLIED – 1700W

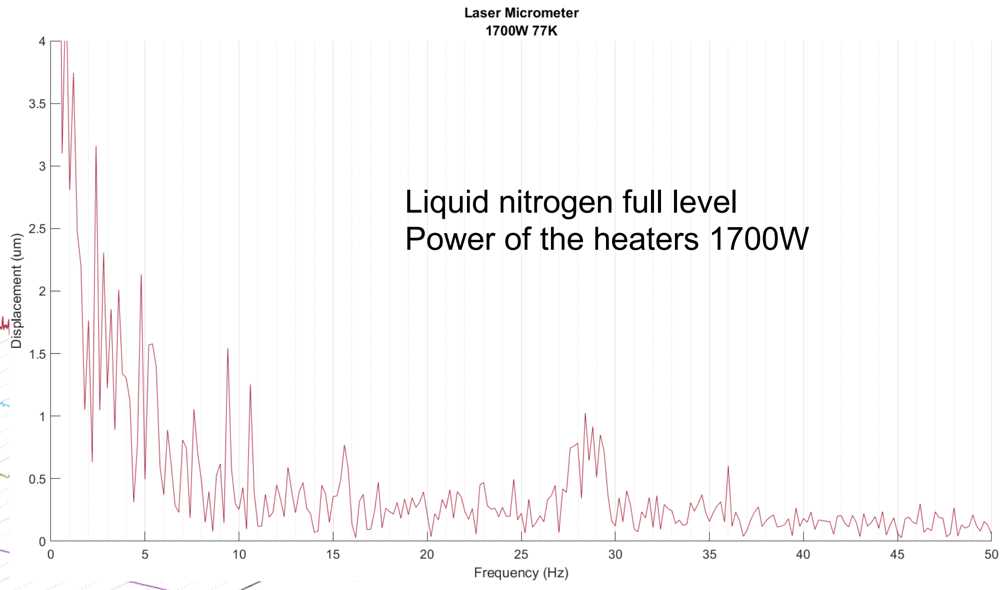

Beam Dynamics Study

- A staged R&D plan that will culminate in the construction of a 3 cryomodule linac with the cryomodules being pre-production prototypes.
  - Fed by an S-band rf photo-injector with a magnetic bunch compressor.
- Injector and diagnostic line
  - Different injector consideration: high charge for beam loading studies; and low charge for structure alignment studies
  - Beam diagnostics is important for overall understanding of the beam dynamics
- Demo facility to study trains of the electron bunches recurring at 120 Hz.
  - Each train to have 133 bunches with the bunch charges of 1 nC separated by: 5 ns for C^3 250 and 3 ns for C^3 550

Beam Dynamics Study

Rendering of the 9 m C^3 cryomodule with 8 one meter accelerating structures, 4 two-meter support rafts, 4 permanent magnetic quadrupoles and integrated beam position monitors.

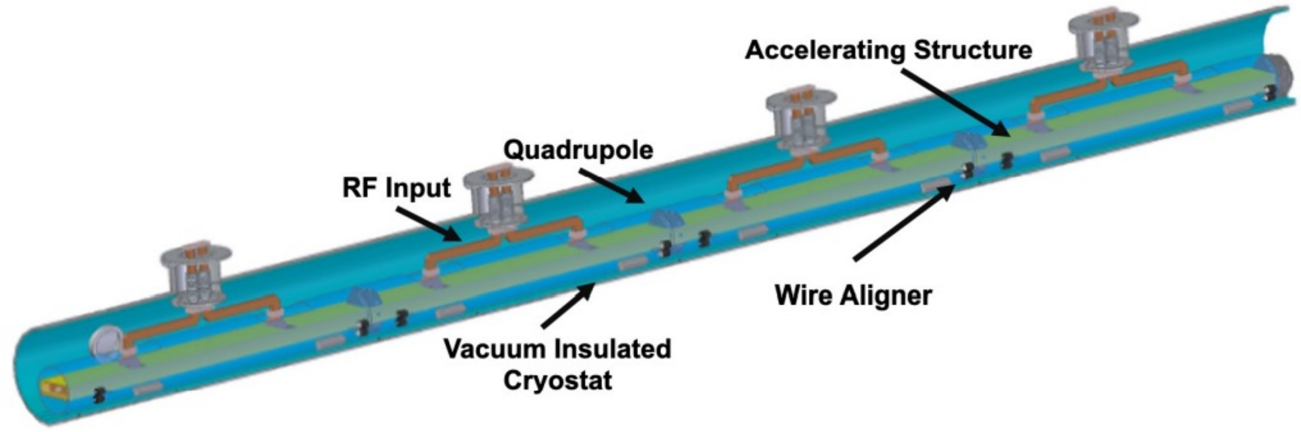

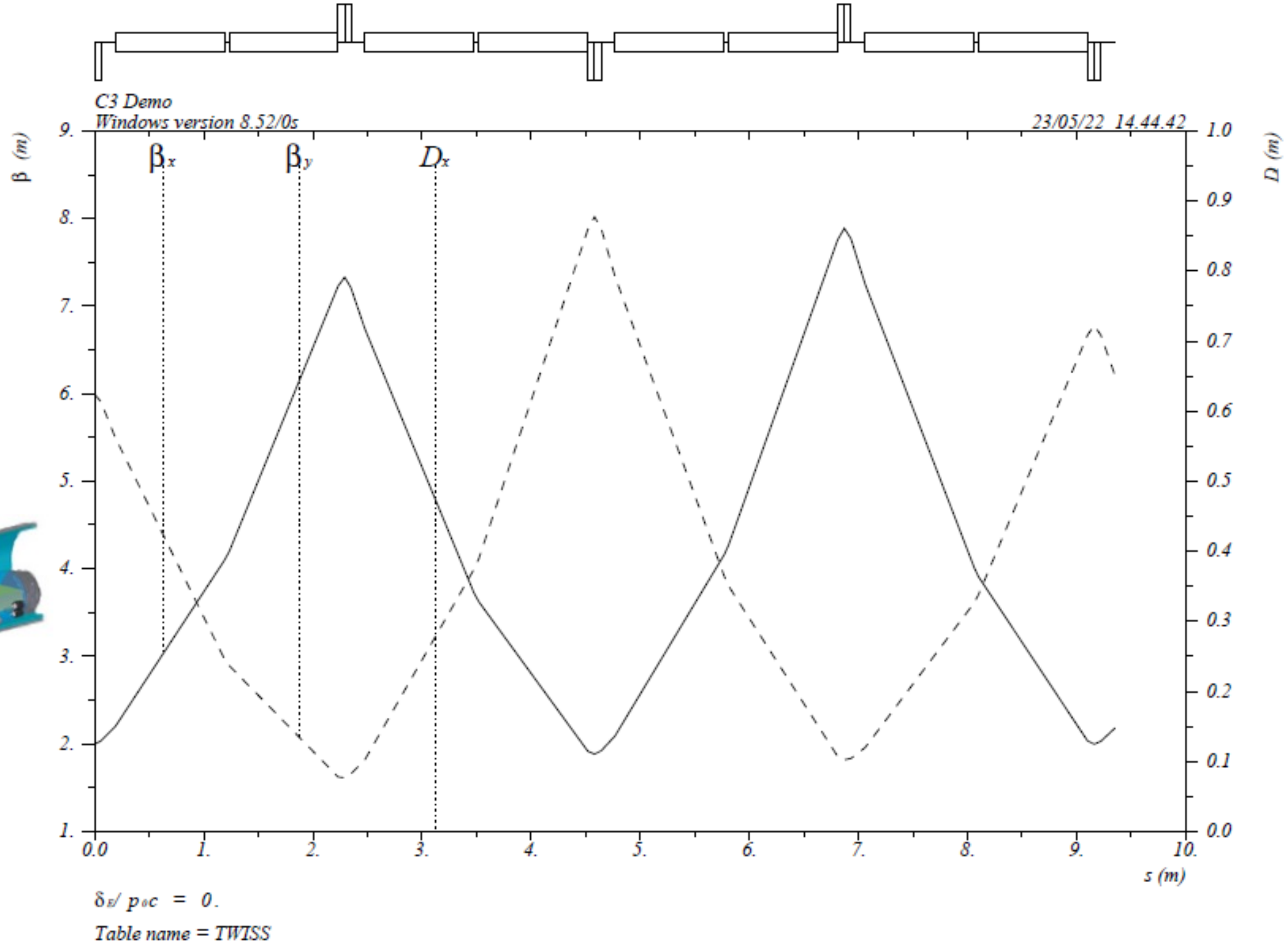

Beam Dynamics Study

- The small diameter of the iris aperture of $a/\lambda = 0.05$ can result in significant short range wake effects
  - Lengthening the bunch length to have $\sigma_z = 500\ \mu\text{m}$
    - Shown in the low right plot, the horizontal axis is the electron injection offset
  - Vary the quadrupole strength to vary the beam size : 200 MeV about 3 T/m
- Achieve a residual energy spread in the range of $\sigma_{\delta 0} = 2 - 5 \times 10^{-3}$ and a maximum of 1% correlated energy spread for Balakin-Novokhatski-Smirnov (BNS) damping
- Design of the structure's damping and detuning to mitigate the effects of long range wakefields
  - Suppress kick factor below 1 V/pC/mm/m

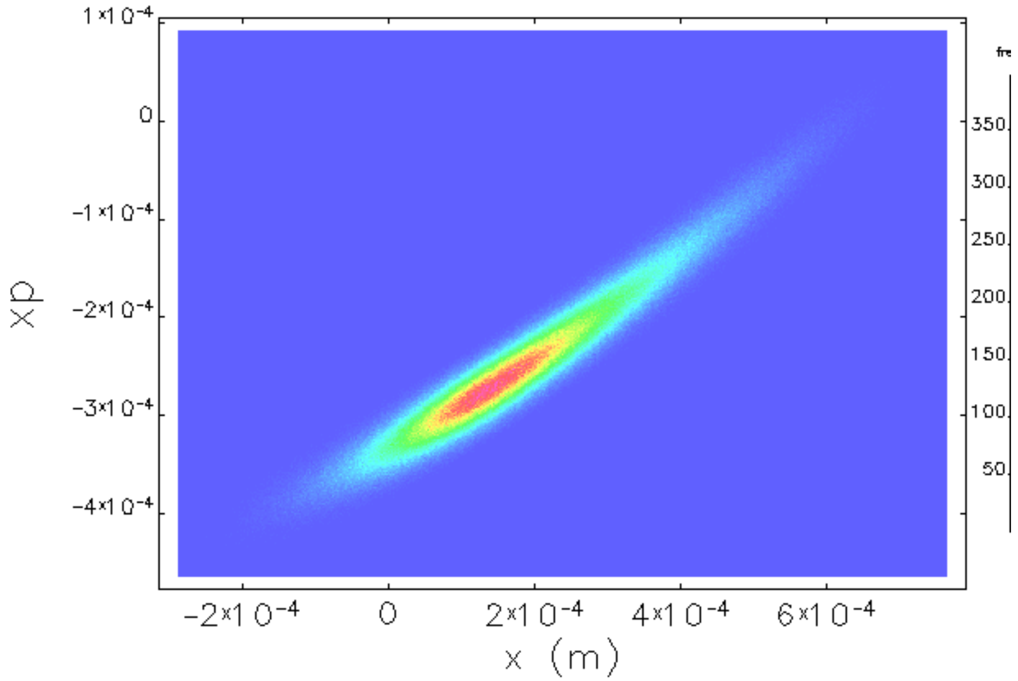

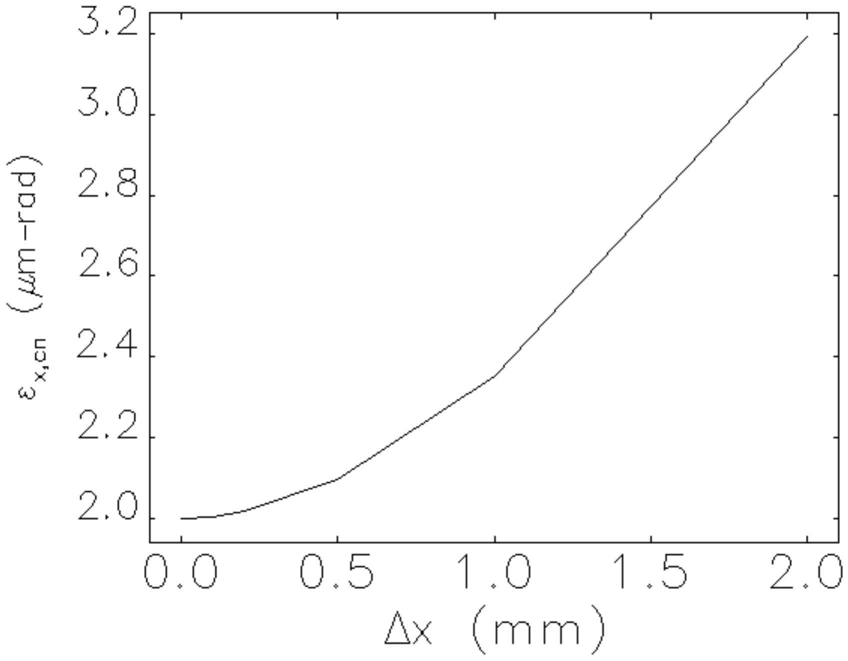

Distributed Coupling Linac for High Charge Electron Bunches

Ankur Dhar, Mohamed Othman, Glen White, Zenghai Li,
Mei Bai, Sami Tantawi, Emilio Alessandro Nanni

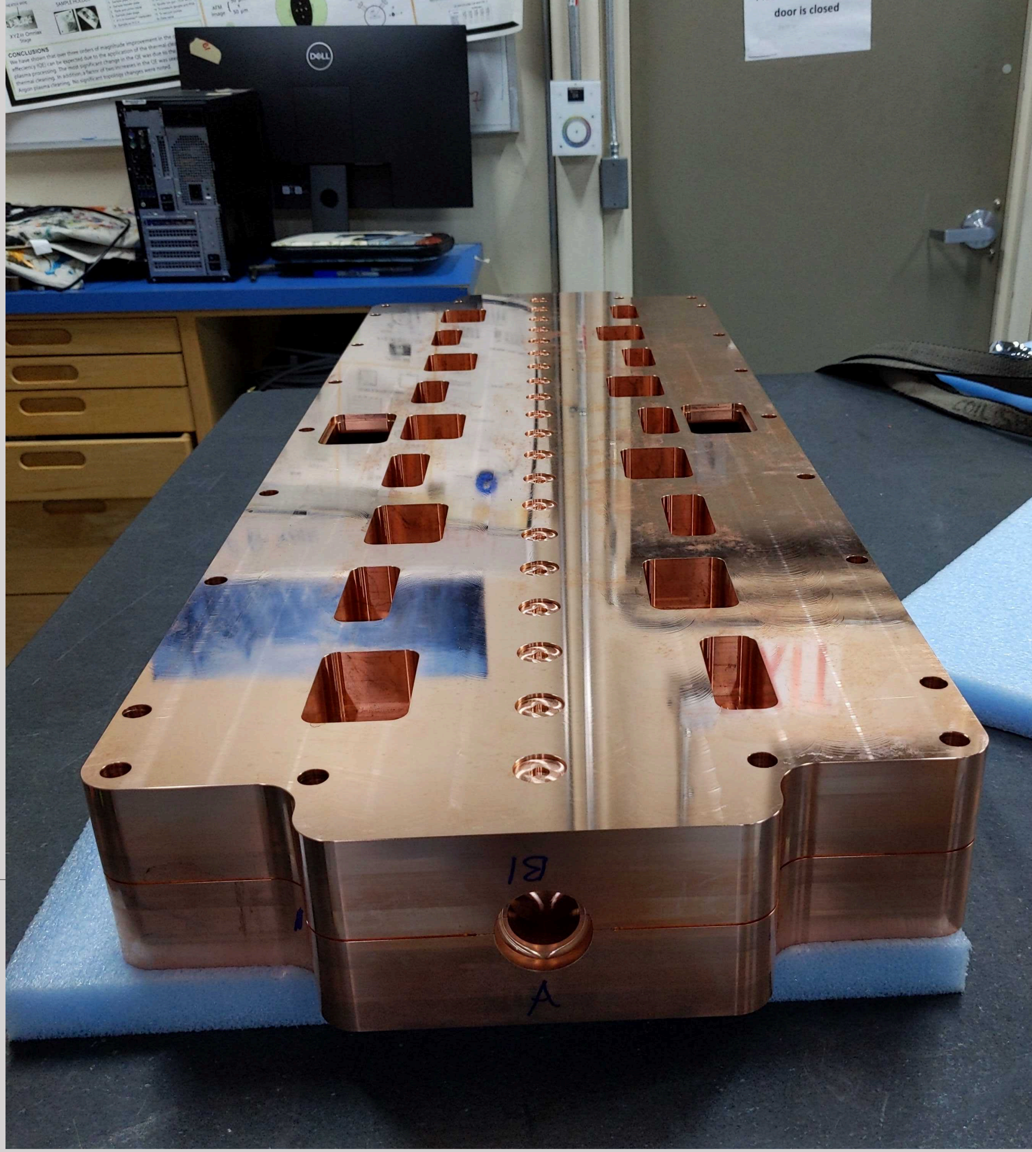

Distributed coupling was applied to injector design

- Design balances shunt impedance with aperture size
  - S-band cavities designed with aperture ratio λ/a=0.135
- Structure is formed from two slabs brazed together
- Better output emittance compared to baseline traveling wave structures

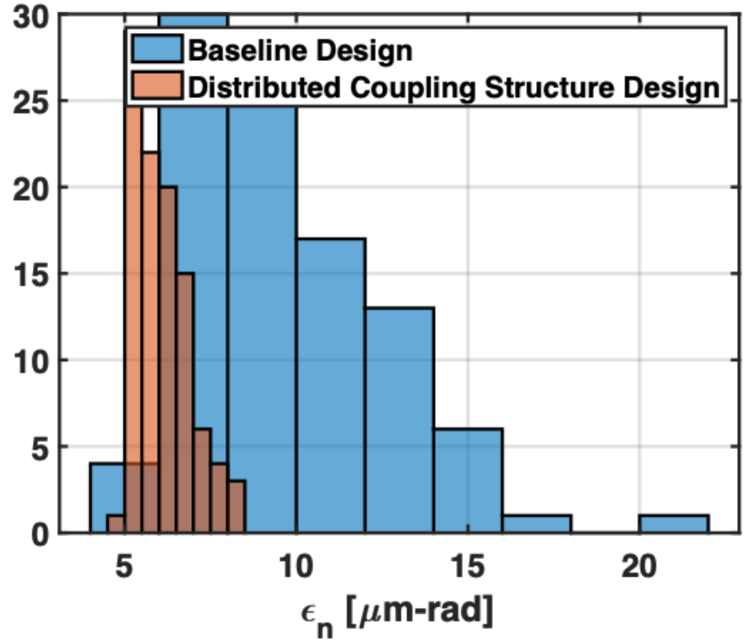

Linac Properties at 5 MW

Frequency	2.856 GHz
Aperture	14.12 mm
a/λ	0.135
E_{max}/E_{acc}	2.63
E_{acc}/Z_0H_{max}	0.995

At 300K

R_s	60 MΩ/m
E_{acc}	16 MV/m

At 80K

R_s	210 MΩ/m
E_{acc}	30 MV/m

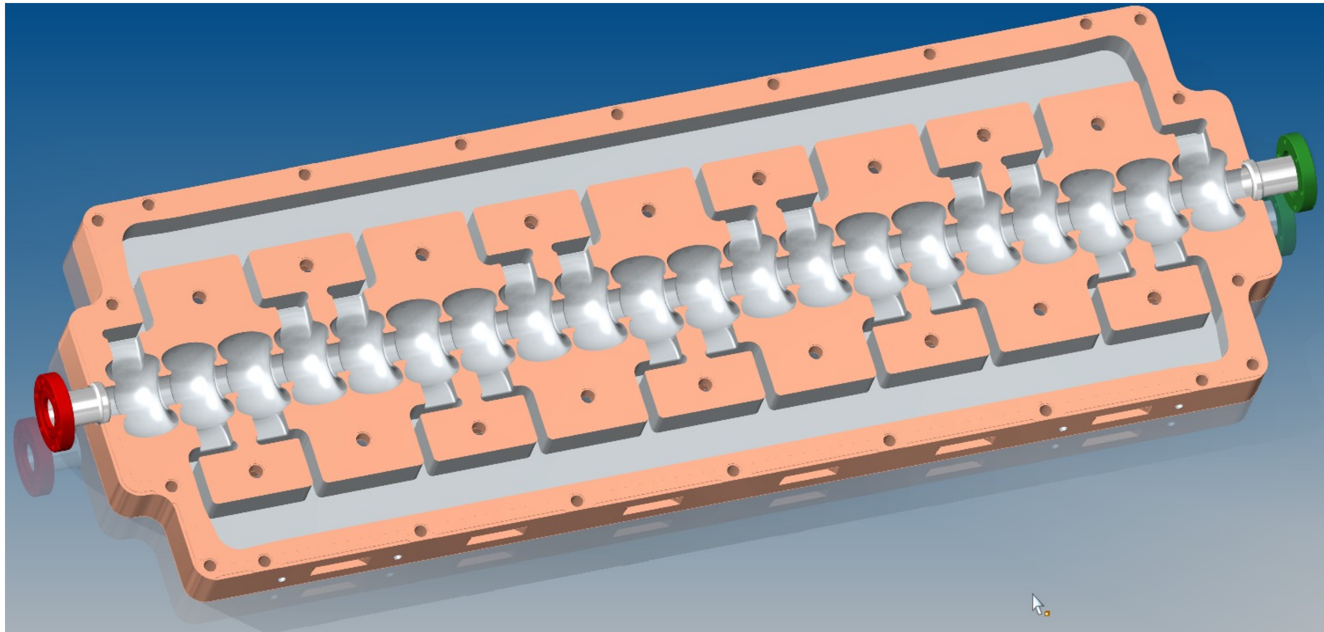

Assembly and characterization are underway

- Linac slabs have been fabricated
- Initial cold tests show coupling between cells into collective modes
- Pi mode converges on operating point quickly, and remains stable

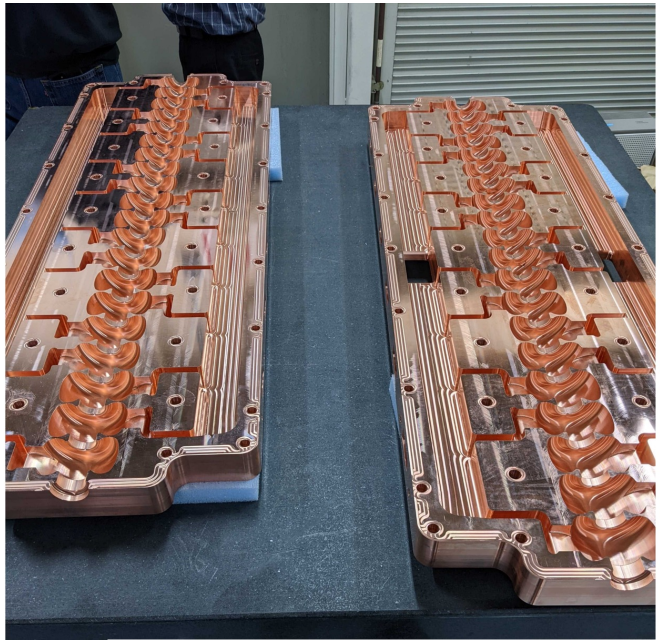

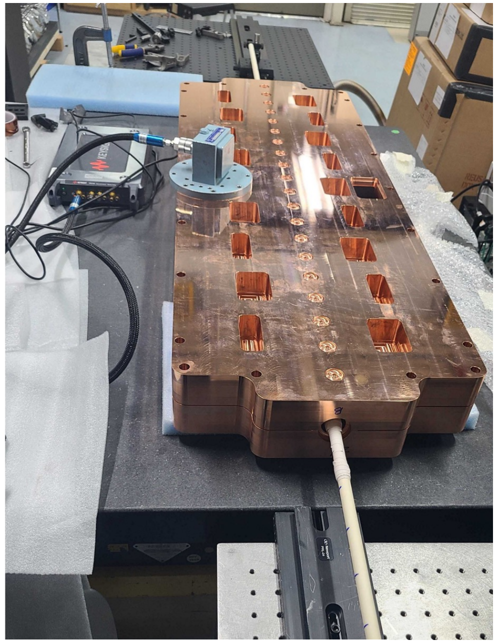

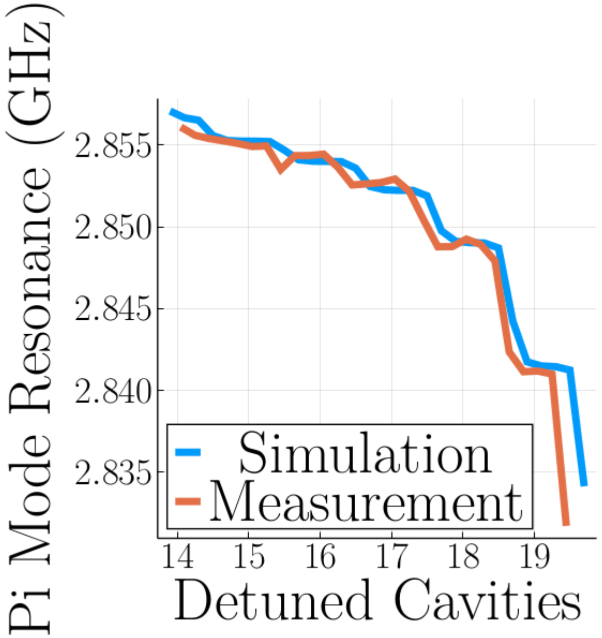

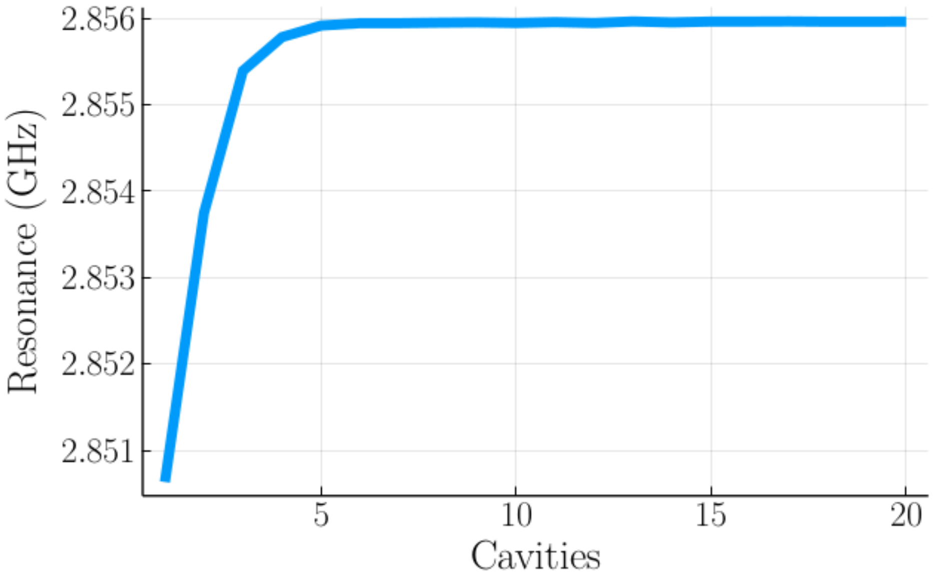

Temperature profile with 80K LN2 nucleate boiling on all outer surfaces

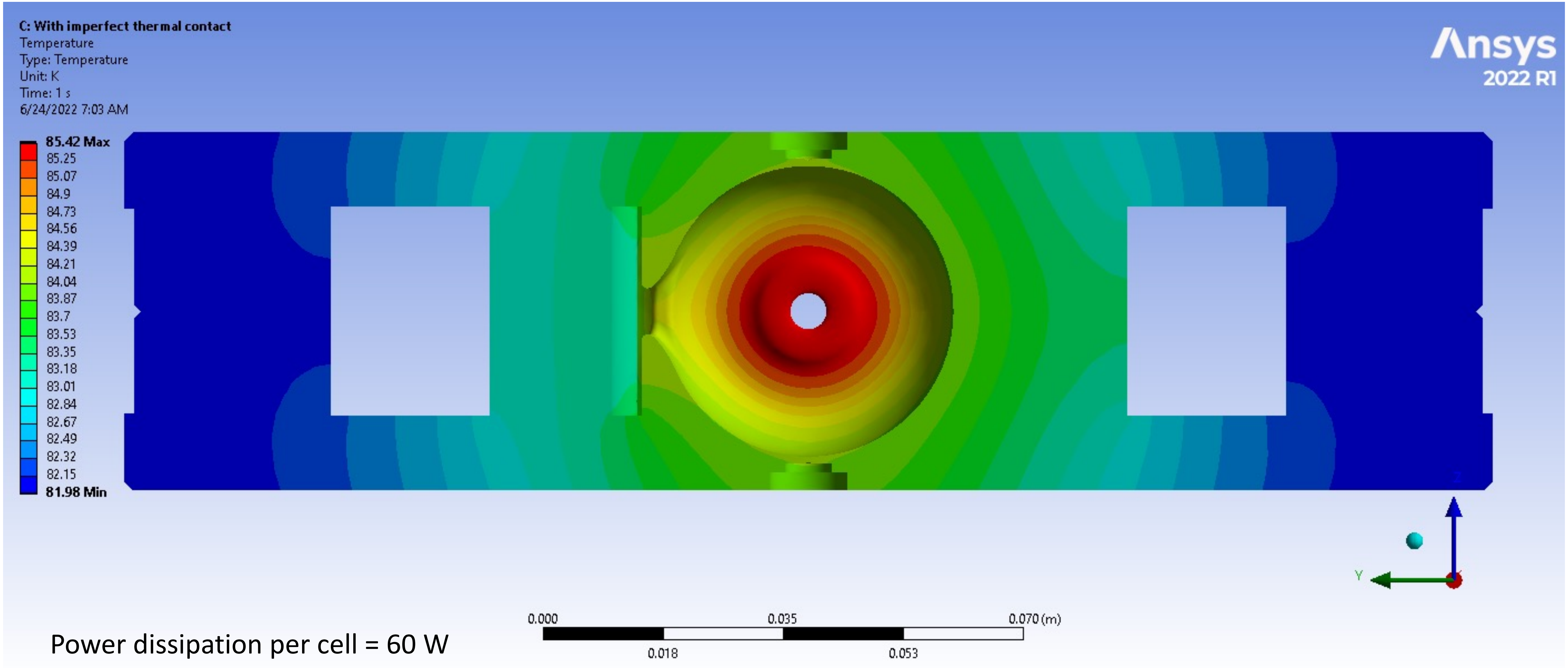

Power dissipation per cell = 60 W

Temperature profile with 80K LN2 nucleate boiling on top and side surfaces only

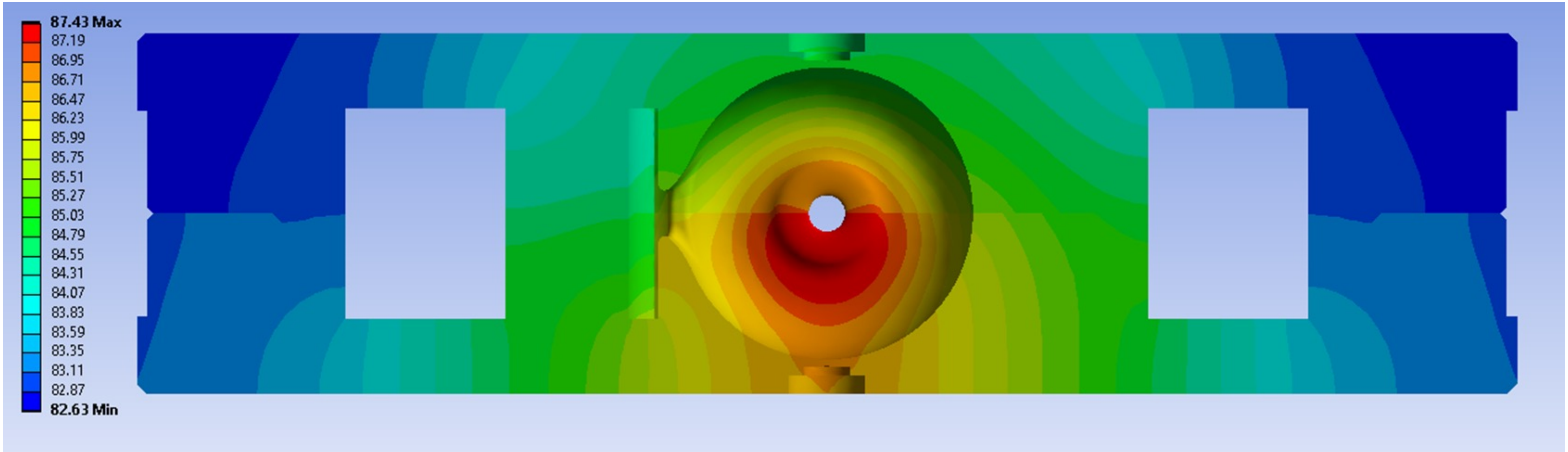

Power dissipation per cell = 60 W